



Published in final edited form as:

*Gastroenterology*. 2016 June ; 150(7): 1545–1557.e2. doi:10.1053/j.gastro.2016.03.040.

## Mounting Pressure in the Microenvironment: Fluids, Solids, and Cells in Pancreatic Ductal Adenocarcinoma

Christopher C. DuFort<sup>1</sup>, Kathleen E. DelGiorno<sup>1</sup>, and Sunil R. Hingorani<sup>1,2,3</sup>

<sup>1</sup>Clinical Research Division, Fred Hutchinson Cancer Research Center, Seattle, Washington

<sup>2</sup>Public Health Sciences Division, Fred Hutchinson Cancer Research Center, Seattle, Washington

<sup>3</sup>Division of Medical Oncology, University of Washington School of Medicine, Seattle, Washington

### Abstract

The microenvironment influences the pathogenesis of solid tumors and plays an outsized role in some. Our understanding of the stromal response to cancers, particularly pancreatic ductal adenocarcinoma, has evolved from that of host defense to tumor offense. We know that most, although not all, of the factors and processes in the microenvironment support tumor epithelial cells. This reappraisal of the roles of stromal elements has also revealed potential vulnerabilities and therapeutic opportunities to exploit. The high concentration in the stroma of the glycosaminoglycan hyaluronan, together with the large gel-fluid phase and pressures it generates, were recently identified as primary sources of treatment resistance in pancreas cancer. Whereas the relatively minor role of free interstitial fluid in the fluid mechanics and perfusion of tumors has been long appreciated, the less mobile, gel-fluid phase has been largely ignored for historical and technical reasons. The inability of classic methods of fluid pressure measurement to capture the gel-fluid phase, together with a dependence on xenograft and allograft systems that inaccurately model tumor vascular biology, has led to an undue emphasis on the role of free fluid in impeding perfusion and drug delivery and an almost complete oversight of the predominant role of the gel-fluid phase. We propose that a hyaluronan-rich, relatively immobile gel-fluid phase induces vascular collapse and hypoperfusion as a primary mechanism of treatment resistance in pancreas cancers. Similar properties may be operant in other solid tumors as well, so revisiting and characterizing fluid mechanics with modern techniques in other autochthonous cancers may be warranted.

### Keywords

Pancreatic Ductal Adenocarcinoma; Interstitial Pressure; Hyaluronan; Gel Fluid; Drug Delivery

---

**Reprint requests.** Address requests for reprints to: Sunil R. Hingorani, MD, PhD, Fred Hutchinson Cancer Research Center, 1100 Fairview Avenue North, M5-C800, Seattle, Washington 98109-1024. srh@fhcrc.org.

### Supplementary Material

Note: To access the supplementary material accompanying this article, visit the online version of *Gastroenterology* at [www.gastrojournal.org](http://www.gastrojournal.org), and at <http://dx.doi.org/10.1053/j.gastro.2016.03.040>.

### Conflicts of interest

The authors disclose no conflicts.

Epithelial malignancies are responsible for most cancer-related deaths worldwide.<sup>1</sup> Named after the organs in which they originate, these carcinomas frequently disseminate and colonize distant organ sites, after which cures are rare, if not impossible. At their most lethal, carcinomas manifest as systemic diseases, not only through metastasis but also by perturbing physiological homeostasis indirectly through neoplastic syndromes and by co-opting other cell types in the body to support their own growth, survival, and spread.<sup>2</sup>

The neo-organ manifested by an emergent carcinoma is an intricate multicellular and multicomponent system. Perhaps nowhere is the tumor microenvironment more robust and complex than in pancreatic ductal adenocarcinoma (PDA).<sup>3</sup> Recognized for almost 2 centuries by its intense desmoplasia, or fibroinflammatory reaction, pancreas cancers typically contain a minority of tumor epithelial cells amid a multitude of immune cells, fibroblasts in various states of activation, and relatively few vessels, embedded within a dense extracellular matrix (ECM).<sup>4,5</sup> Initially viewed as an ultimately futile host defense, we now know that many, although not all, of these stromal elements support tumorigenesis.<sup>6-9</sup> The study of the fluids, solids, and cells in this microenvironment is therefore essential to understanding the pathogenesis of PDA and could also provide the means to its end.

We review how fluids conspire with solids and cells to resist treatment of pancreas cancer. Specifically, we describe mechanisms behind the substantial increases in interstitial pressures in PDA, which can greatly exceed mean vascular pressures and compromise the efficacy of traditional chemotherapeutics.<sup>10,11</sup> Targeted enzymatic degradation of hyaluronic acid (HA) reverses these increases in pressure, allowing collapsed vessels to reopen and improving perfusion.<sup>10,12</sup> Despite extensive studies of interstitial fluid pressure (IFP) that have spanned more than half a century, the sources of pressures most germane to impaired solute delivery in solid tumors are still debated, as are the most accurate ways to characterize and measure them.<sup>13</sup> We review the most common methods of pressure measurement and propose a model to reconcile existing terminologies and concepts. We also compare the abilities of experimental systems to accurately recapitulate the essential biophysical features of autochthonous PDA and evaluate their benefits and limitations in translating potential strategies for clinical application.

## Basic Principles

Solutes, nutrients, and intravenously administered drugs are delivered to tissues by 2 main passive processes: diffusion, driven by concentration gradients between the vascular and extravascular (interstitial) spaces, and convection, driven by pressure gradients between the same 2 compartments. The widespread vascular collapse characteristic of PDA compromises diffusion and convection, hindering the delivery of chemotherapeutic agents to the tumor bed. The forces underlying these 2 processes, in turn, derive from fundamental thermodynamic principles involving the movement of fluid and solutes across a semipermeable membrane. There are numerous excellent reviews of this subject, so only a few salient features will be revisited here.<sup>14-16</sup>

The passive transport processes of biological membranes are often illustrated through an ideal 2-compartment system separated by a semipermeable membrane that restricts

macromolecular diffusion but permits fluid to partition freely (Supplementary Figure 1). One side is filled with fluid plus the macromolecule and the other with fluid only. The second law of thermodynamics dictates that the system will change to reach a state of minimal free energy, in other words, to equilibrate the chemical potential of water ( $\mu$ ) on both sides. In state 1,  $\mu(A) < \mu(B)$  and this difference provides the force for fluid movement from side B to side A. If both sides are allowed to expand and contract at constant pressure and temperature (eg, a system open to the atmosphere), equilibrium will never be reached because the chemical potential difference of water on the 2 sides ( $\mu_B - \mu_A$ ) will always be positive and water will move from side B to side A until side B empties. Let us propose instead that the total volume on side A is restricted (state 2); in this case, water will move from side B to side A until a pressure difference,  $DP = (P_A - P_B)$ , develops sufficient to balance the chemical potential of water on both sides. This pressure difference is defined as the osmotic pressure, and the example provides a concrete way to think about the osmotic pressure of a particle at a given concentration; it is equivalent to the increase in hydrostatic pressure required to equilibrate the chemical potential of water on both sides of the semipermeable barrier. It should be noted that processes in living systems are never at true thermodynamic equilibrium (which requires that neither matter nor energy enter or leave the system); they can, however, often be found at steady state, and the fundamental principles of thermodynamics still govern the outcomes.

Pancreas cancers exist in a mechanically unbalanced state due to high interstitial concentrations of HA, avid binding of fluid into one or more immobilized states, and subsequent loading of tethered fibrillary networks that respond through contractile forces to maintain cellular homeostasis. Together, these forces engender the widespread vascular collapse that serves as a primary mechanism of drug resistance in PDA. Tissue pressures in the interstitium have historically been categorized as those due to free fluid and those due to solid stress, and multiple factors contribute to each. The measurement of free fluid pressures in normal and neoplastic tissues has a long history and includes well-developed theoretical frameworks to describe the operant principles.<sup>14,17-19</sup> Solid stress, on the other hand, has never been directly measured in autochthonous cancers, although it has been approximated in ex vivo and in vitro experimental and mathematical models (eg, Helmlinger et al,<sup>20</sup> Stylianopoulos et al,<sup>21</sup> and Sarntinoranont et al<sup>22</sup>). However, the largest source of interstitial pressure in pancreas cancers combines properties of fluids and solids and can perhaps be described most informatively as a distinct entity: the viscoelastic gel-fluid phase. We briefly trace the history of investigation into these forces and the principles underlying them and present a unified model that encompasses all 3 sources.

## Interstitial Free Fluid

### Transvascular Fluid Flux

The modern era of tissue fluid pressure measurements in healthy and diseased tissues was launched by the work and theories of Ernest Starling (reviewed by Michel<sup>23</sup>). Originally presented in 1896, these ideas form the basis for understanding the mechanisms of fluid flow into or out of the capillary network and continue to inform studies of tissue fluxes and pressures undergoing a renaissance in the field of cancer biology.<sup>24</sup> To explain the rapid

entry into the circulation of a saline bolus injected into the tissue of an isolated dog hind limb, Starling proposed the presence of an oncotic pressure composed of proteins trapped within the vasculature that led to rapid reabsorption followed by passive redistribution of salts. He excluded back-filtration, that is, the reverse of the process that generated transvascular fluid flux, reasoning that an increase in interstitial hydrostatic pressure would collapse the postcapillary vessels, leading to an immediate increase in capillary pressures that would then oppose any back-filtration. Synthesizing these observations, Starling conjectured that “the osmotic attraction of the serum for the extravascular fluid will be proportional to the force expended in the production of this latter, so that, at any given time, there must be a balance between the hydrostatic pressure of the blood in the capillaries and the osmotic attraction of the blood for the surrounding fluids.”<sup>24</sup> We can summarize Starling’s hypothesis as follows:

$$P_c - P_i \approx \pi_c - \pi_i$$

This formula states that under normal conditions, the net hydrostatic pressure (capillary pressure [ $P_c$ ] minus interstitial fluid pressure [ $P_i$ ]) promotes filtration out of tissue capillaries and is largely counterbalanced by a net intravascular oncotic pressure (capillary oncotic pressure [ $\pi_c$ ] minus interstitial oncotic pressure [ $\pi_i$ ]) that promotes fluid retention.

Several decades passed before direct experimental evidence would substantiate this hypothesis. After methods were developed to estimate fluid fluxes across capillary beds, it was discovered that a plot of fluid flux per unit capillary surface area ( $J_v/A$ ) versus capillary pressure ( $P_c$ ) was linear and that the 0 intercept (ie, the  $P_c$  at which there was no net fluid flux) was roughly equal to the plasma oncotic pressure ( $P_O$ ). At pressures above that value, a net efflux of fluid (filtration) was observed; at pressures below, fluid was absorbed. The constant of proportionality (the slope of the line) was the hydraulic permeability of the capillary wall ( $L_p$ ), which can vary depending on the properties of the vessel, the presence of inflammatory or ischemic injury, and so on. We can therefore more closely approximate these relationships as follows:

$$\frac{J_v}{A} \approx L_p((P_c - P_i) - (\pi_c - \pi_i)).$$

The ability of macromolecules to generate oncotic pressure depends also on the permeability of the vessel wall to that substance (ie, the extent to which the macromolecule is retained in a given compartment). The reflection coefficient,  $\sigma$ , varies from 1 (fully retained) to 0 (fully permeant).<sup>17–19</sup> Each osmotically active solute contributes to the osmotic pressure difference as modified by its unique reflection coefficient. Thus, the total osmotic pressure difference can be written as the sum of the contributions from each individual solute:

$$\sigma_1 \Delta \pi_1 + \sigma_2 \Delta \pi_2 + \dots + \sigma_n \Delta \pi_n = \sum_{r=1}^n \sigma_r \Delta \pi_r.$$

Putting all of these observations and parameters together, we obtain the full Staverman–Kedem–Katchalsky equation:

$$\frac{J_v}{A} = L_p \left( \Delta P - \sum_{r=1}^n \sigma_r \Delta \pi_r \right).$$

With this equation, Starling's hypothesis becomes a principle.<sup>23</sup>

In summary, the movement of water between capillaries and the interstitial space is determined by the difference in the chemical potential of water,  $\mu$ , across the 2 compartments; osmotically active molecules decrease  $\mu$ , which is counter-balanced by increases in hydrostatic pressure (Supplementary Figure 1). The factors that contribute to the movement of water into and out of capillaries are therefore the hydrostatic and oncotic pressures as well as the physical characteristics of the capillary wall itself. The Starling equation can be seen as an expression of the second law of thermodynamics in defining the factors that promote and respond to differences in the chemical potential of water on either side of a semipermeable membrane.<sup>24</sup> Starling would later apply these ideas to studies of the pathophysiological accumulation of interstitial free fluid (or lymph) known as dropsy, or edema.<sup>24-26</sup> This concern would continue to occupy physiologists for the next half century who, in turn, would also develop methods to measure these free-fluid pressures.

### Classic Methods of Measurement

Early techniques for measuring free IFP involved the insertion of a needle or capillary pipette into tissue and determining the minimum pressure required for fluid to flow from the needle into the interstitial space.<sup>27</sup> However, even the smallest-diameter needles are 300 to 500 times larger than the widths of interstitial spaces, which are typically less than 1  $\mu\text{m}$ , and can therefore cause tissue distortions that introduce errors in measurements. The needles also cause inflammatory responses and local swelling, altering the phenomenon to be measured. To minimize these variables, Guyton pioneered a technique by implanting perforated capsules into tissues and allowing sufficient time to reach steady state (typically 2-3 weeks) (Figure 1A).<sup>28</sup> A needle was then inserted into the capsule through one of the perforations into the inner cavity to measure the absorption pressure, or free IFP. The larger surface area of contact and time for equilibration between the device and fluid in the interstitial space makes the perforated capsule perhaps the most accurate of the classic methods to measure the free-fluid phase pressures in normal tissues.

A more rapid and simple method for measuring IFP in animal tissues was developed using a capillary tube fitted with a cotton wick.<sup>29</sup> In this technique, a wick is pulled through the end of Teflon tubing, a glass tube inserted into the other end, and the assembly filled with saline and fitted with a hypodermic needle. After insertion into the tissue, the needle guide is pulled back so that the tubing and wick make direct contact with the interstitial space. The wick establishes continuity with the tissue fluid, and the meniscus in the capillary is balanced with a manometer. This technique was further elaborated to become one of the early standards of free IFP measurement, called the wick-in-needle (WN) (Figure 1B).<sup>30</sup> Modifications included a 2- to 4-mm-long side port and replacing the cotton wick with several multi-filamentous nylon threads. This configuration was designed to prevent obstruction at the tip, as occurred with other needle-based techniques. A crucial limitation of

these needle and other fluid equilibration techniques is that they make accurate measurements only in the presence of abundant fluid, flowing freely in continuous channels, as occurs in cases of edema. Normal tissues typically contain small amounts of free fluid, if any, and even then only in isolated regions or pockets.<sup>27</sup>

Pressures measured with the WN and implanted capsules in most tissues are slightly negative relative to atmosphere; these pressures are also lower than the slightly positive pressures typically measured with the micropipette.<sup>28</sup> This discrepancy led to invoking the presence of a solid tissue pressure from compacted tissue elements and the supposition that the micropipette measured a combination of fluid and solid tissue pressures (ie, the bleb of fluid at the tip of the micropipette was postulated, in effect, to separate the tissue planes and allow fluid to then flow, so the instrument actually measured a type of tissue resistance).<sup>27,31</sup> Aukland and Reed correctly pointed out that the negative fluid pressure can only occur if “the interstitium exists in a dehydrated state.”<sup>32</sup> This dehydrated state is maintained by lymphatic flow and unsaturated HA. For freely mobile fluid to increase substantially, interstitial glycosaminoglycans (GAGs) such as HA would either have to be excluded or be saturated.<sup>13,33</sup> These investigators concluded that in most normally hydrated tissues, solid tissue pressures were largely negligible and could thus be ignored.<sup>32</sup>

### Classic Models and Mechanisms

The first measurements of fluid pressures in cancer were performed by Young et al,<sup>34</sup> who used the needle technique in testicular allografts of Brown–Pearce carcinoma cells<sup>35</sup> to test their hypothesis that increased extravascular pressures promote the intravasation and metastasis of cancer cells. Various classic methods of pressure measurement were subsequently applied to a variety of xenograft, allograft, and in vitro tumor model systems.<sup>36</sup> A large amount of work and several theoretical frameworks have therefore been constructed around transplantable and other artificial model systems, which differ in fundamental respects from autochthonous cancers (Figure 2).<sup>37</sup> These systems are characterized by abnormal and fenestrated (leaky) vessels attributed to rapid neoangiogenesis and vascular endothelial growth factor–induced hyperpermeability.<sup>38</sup> These experimental platforms, together with the use of classic fluid equilibration techniques that can measure only free fluid, have understandably led to descriptions of modestly increased IFPs in cancers. These result primarily from perturbations in vascular architecture and biology as well as a redistribution across the vessel wall of oncologically active molecules from the circulation.<sup>39</sup>

Tumor vessels associated with PDA<sup>12</sup> lack the fenestrations and open interendothelial junctions characteristic of these transplantable tumor model systems<sup>40</sup> and therefore have low free-fluid IFPs. The free-fluid pressures measured by the WN in autochthonous PDA<sup>11,41</sup> are even lower than those measured in xenografts or allografts. Despite the exhaustive studies of free-fluid pressure in these systems,<sup>42,43</sup> findings from these studies have produced a conceptual framework with little ability to explain the biophysical challenges in PDA.<sup>44–47</sup> It is therefore reasonable to assume that interstitial pressures may have been underestimated in other solid tumors as well.

Limitations in the generalizability of earlier experimental platforms to autochthonous cancers across a number of physiological and molecular parameters<sup>48–51</sup> motivated and



justified the development of genetically engineered mouse models. Genetically engineered mouse models of PDA develop spontaneous tumors that manifest many important features of the human disease, permitting rigorous studies of disease initiation, progression, and pathophysiology.<sup>52–55</sup> In contrast to mice with subcutaneous tumors, *Kras*<sup>LSL-G12D/+;Trp53<sup>LSL-R172H/+</sup>; Cre (KPC)</sup> mice develop pancreatic tumors with a highly desmoplastic stroma and lower mean vessel densities and cross-sectional luminal areas. These combine to severely limit diffusion of chemotherapeutics and reveal a principal mechanism of drug resistance common to murine and human autochthonous PDAs.<sup>9,52–54</sup> These genetically engineered mice have enabled detailed explorations of the role of matrix constituents as barriers to treatment (Figure 2).<sup>56</sup>

## Interstitial Gel Fluid

### Fluid Mechanics

Most interstitial fluid is not free flowing but rather exists in complex with GAGs and proteoglycans, generating a relatively immobile gel-fluid phase. It has been estimated that less than 1% of total tissue interstitial fluid is freely mobile,<sup>57</sup> explaining why incising tissues releases no freeflowing fluid (aside from the vasculature).<sup>29</sup>

The principal interstitial GAG is HA, a high-molecular-weight polysaccharide originally isolated from the vitreous body of the eye.<sup>58</sup> HA is present in the extracellular and pericellular matrices of most organs and contributes to tissue hydration, architecture, and elasticity.<sup>59</sup> It was postulated more than 50 years ago that water could form the basis of a tissue structure resistant to compressive forces if its free flow could be hindered.<sup>60</sup> The unique properties of HA arise from its anionic, nonsulfated, and unbranched structure composed of repeating disaccharide units of *N*-acetylglucosamine and *D*-glucuronic acid. This megadalton polymer has the astonishing ability to bind and organize up to 15 water molecules per disaccharide. As a result, hydrated HA can swell to 1000-fold its solid volume to a coil diameter of approximately 600 nm.<sup>61–63</sup> HA strongly affects fluid flow and pressures; fluid movement is impeded by a factor of  $\sim 10^7$  in the presence of a 1% HA solution in a 0.1-mm capillary tube.<sup>64</sup> This ability of hydrated HA to resist compression forms the basis of its shock-absorbing properties in the joint space. However, HA can also expand as a result of electrostatic repulsion along its highly negatively charged surface to generate significant swelling pressures.

Hydrated HA generates pressures associated with the free fluid within it, osmotic pressures (including contributions from the Gibbs–Donnan effect), oncotic pressures from its ability to organize water into several distinct gel-fluid phases, and a swelling pressure that results from electrostatic repulsion across the concentrated negative surface charge.<sup>27,65–68</sup> This gel-like phase also has a modulus of elasticity and, so can interact with and transmit solid tissue pressure similar to “the actual structural solids of the tissue spaces.”<sup>27</sup> However, this captures only part of the picture. This gel-fluid phase also has viscosity, a property of fluids, and solutions of HA exhibit normal Newtonian behavior across a wide range of concentrations and shear rates.<sup>69</sup> The interstitial gel-like fluid phase, mainly comprising hydrated HA, and its interactions with collagen and microfibrillary networks, is therefore most accurately described as a viscoelastic (Figure 3). These properties become especially

important when considering the different ways that forces are transmitted through fluids and solids (see the following text).

Finally, where does the energy driving the swelling pressure come from? Based on the thermodynamic principles discussed in the preceding text, we surmise that the energy comes from the decrease in chemical potential of water in the interstitium due to the high concentrations of interstitial HA. This can also be thought of as the binding energy of water in complex with HA which, together with the negative surface charge, induces a conformational change expanding its effective volume; this expansion applies a tensile load on the microfibrillary network, which contracts in response, and the resulting increase in pressure restores the chemical potential of the water.

### Measuring Gel Fluid Pressures: Piezoelectric Pressure Catheters

As Brace<sup>13</sup> and others<sup>28,32,68</sup> have noted, “there appears to be an exceedingly small amount of free fluid in many tissues under conditions of normal hydration, if there is any at all.”<sup>13</sup> Partly as a result, the major pathological condition of concern for many decades was edema. Moreover, given that all of the instrumentation available at the time for measuring tissue fluid pressure (including WN) could measure only the free-fluid phase,<sup>13</sup> the immobile gel-fluid phase was not detected.

A novel technique was more recently introduced that does not rely on copious free fluid to measure pressures and involves a polyurethane transducer-tipped pressure catheter (PC) (Figure 1C). The PC uses a piezoelectric membrane recessed in a side port to sense fluid pressure and is known for unimpeachable accuracy in the range of  $-50$  mm Hg to  $+300$  mm Hg.<sup>70,71</sup>

One theoretical concern about this instrument is the potential occlusion by solid elements, which could introduce artifacts reflecting solid stress. We place the PC in the lumen of a small-gauge surgical guide needle and then insert the assembly into the tissue as the needle sleeve is withdrawn. This method, together with a recessed sensor in a side port location, minimizes the likelihood of direct contact with solid tissue components. We have shown that a reconfigured PC-in-needle (ie, a PC sheathed inside a needle to shield it from solid tissue) gave the same readings as the PC itself, excluding the possibility of solid pressure artifacts in this context.<sup>11</sup>

These concerns had been previously addressed by Ozerdem and Hargens, pioneers in the use of the PC, who found no evidence for solid tissue pressure artifacts in their work on tumor xenografts.<sup>71</sup> The device has since been successfully used to measure tumor IFP in a variety of systems.<sup>10,71-74</sup> The PC therefore records pressure accurately in both the free- and gel-fluid phases.

### Signaling Properties

This review is primarily concerned with the physicochemical properties of the interstitium and the barriers to delivery of drugs for pancreas cancer. However, it should be noted that HA participates in the modulation of many physiological processes via force generation and direct signaling. Several cell surface receptors bind directly to HA to activate pathways that



affect development, wound healing, mitosis, oncogenesis, and migration.<sup>58,59,75</sup> The principal HA-binding receptors that have been identified include CD44, RHAMM, LYVE1, IVd4, LEC, and ICAM1.<sup>76,77</sup> CD44 and RHAMM, which are frequently overexpressed in a number of solid tumors, are the most studied and are key regulators of inflammation and metastasis.<sup>78</sup>

The mechanical forces exerted by HA during swelling figure prominently in normal biology and pathophysiology and have garnered attention in other fields such as cosmesis.<sup>79</sup> Deposition of HA and proteoglycans into the ECM during development generates hydrostatic swelling pressures that promote morphogenesis. For example, the normal development of the secondary palate shelf during embryogenesis requires HA-induced mechanical cues. When HA deposition is disrupted by exposure to chlorcyclizine, the palate shelf curves incorrectly and develops with a smaller volume.<sup>80</sup> Similar HA-dependent mechanical pressures affect the development of the ciliary body and the correct positioning of the anterior retina and corneal structure.<sup>81–83</sup> From these, among many other examples, one can postulate that perturbing these mechanisms of force generation and cell signaling might have important implications in cancer biology.<sup>79</sup>

## Solids and Cells

Collagen fibers are the principal structural element in tissues and absorb compressive stresses, whereas the interstitial gel fluid and free fluid distribute hydraulic pressure. Hydrated HA generates multiple types of osmotic and oncotic forces, which combine with electrostatic repulsion to create a substantial swelling pressure. Expansion of the interstitial gel fluid against the collagen–microfibril network places it under tension rather than compression. When the gel-fluid phase predominates, as in PDA, the fluid-like viscoelastic properties become the primary determinant of force generation and can exert a considerable tensile load on collagen fibers tethered to cells. Within the confines of collagen-dense tumors, the reciprocal contractile force generated by cells in the attempt to maintain tensional homeostasis allows interstitial pressures to increase still further. The net pressures generated depend not only on the density of fibrillar collagen but also on the orientation of these fibrils relative to the applied load and the compliance of the tissue.

Cancers also co-opt normal tissue repair processes, resembling wounds that do not heal.<sup>84</sup> Normal fibroblasts contribute to the structural integrity and architecture of tissues through the formation and maintenance of the ECM.<sup>85</sup> When subverted during tumorigenesis to become cancer-associated fibroblasts, these activated cells deposit excessive ECM components, including collagen I and III, fibronectin, and HA, which help shape the emerging neo-organ and promote the survival and dissemination of cancer cells.<sup>86</sup> Targeting cancer-associated fibroblasts, either by depletion or by reversion to a quiescent state, therefore has the potential to reestablish the growth-restraining cues of a normal microenvironment.<sup>9,87–89</sup>

New therapies have emerged to target solid and cellular stromal elements based on the paradigm that the tumor microenvironment supports cancer cell proliferation and survival. Targeted depletion of  $\alpha$ -smooth muscle actin—positive stromal fibroblasts (a marker of

cancer-associated fibroblasts) by the hedgehog inhibitor saridegib (IPI-926) reduced tumor cell proliferation and collagen content.<sup>9</sup> Mean vessel density also increased through stimulation of angiogenesis; when mice were also given gemcitabine, mean vessel density approximated that of the normal pancreatic tissue.<sup>9</sup> Although these effects were short lived, they provided proof of principle that targeted depletion of the stroma can improve drug delivery and efficacy.

However, these studies did not investigate potential long-term effects of this therapeutic approach, and subsequent work has revealed the dangers of corrupting the tumor-restraining properties of stromal elements. Targeted genetic deletion of sonic hedgehog (*Shh*) in mice with pancreatic tumors led to chronic depletion of stromal cells, resulting in increased vascularity and more aggressive tumors with undifferentiated histology.<sup>88</sup> Survival decreased due to accelerated primary tumor growth and metastasis, providing a potential explanation for the reported failure and implied worsening of disease reported from a clinical trial of saridegib plus gemcitabine in patients with pancreas cancer.<sup>90</sup>

Additional strategies are being explored to restore rather than ablate the tumor microenvironment. For example, the vitamin D receptor ligand, calcipotriol, reprogrammed the tumor microenvironment in *KPC* mice by decreasing inflammatory cytokines and collagen deposition, increasing angiogenesis, and inhibiting CXCL12 to restore a T-cell response. The combination of calcipotriol and gemcitabine increased the median survival time of *KPC* mice by 58%, and there was a 29% increase in animals that survived beyond 1 year compared with gemcitabine alone.<sup>89</sup> As a cautionary note, these studies involved only short-term therapy (lasting several days) and the untoward effects, if any, of prolonged vitamin D therapy on the pathogenesis of PDA have not been investigated. Nevertheless, these studies highlighted the complexities and nuances of the components and processes in the tumor microenvironment. Our concept of stromal elements as either beneficial or deleterious must be revised to emphasize strategies that restore the tumorsuppressing properties of the microenvironment and normal tissue homeostasis.

Proliferation and recruitment of cells can also contribute to intratumoral forces and stresses that can alter the activities and responses of signaling pathways and cause blood vessel collapse via mechanical compression.<sup>91</sup> Depletion of tumor cells with diphtheria toxin in xenograft models led to vasculature re-expansion and increased drug delivery.<sup>91</sup> Similar observations were reported with hedgehog inhibition in a xenograft model.<sup>21</sup> It is worth noting, however, that pancreas cancers are hypocellular, particularly with respect to the proliferating epithelial cell compartment. In contrast, xenograft tumors grown from pancreas cancer cells are hypercellular and have short tumor cell-to-vessel distances, inviting the conclusion that growth-induced solid stress from rapidly proliferating tumor cells led to vessel collapse. In autochthonous pancreas cancers, however, the tumor cells are tens of microns away from vessels, making it unlikely that there is sufficient area of direct contact between the vasculature and solid elements to cause widespread vascular collapse.<sup>9</sup>

Solid stress is difficult to measure in these contexts. A creative method was recently adapted to estimate growth-induced solid stress in tumor spheroids grown from a range of cancer cell lines, including PDAs.<sup>21</sup> The cell lines were first grown under the renal capsule of

immunocompromised mice; tumor spheroids were then extracted, glued to a Plexiglas platform, and partially transected with a scalpel.<sup>21</sup> The extent to which the incision expanded was interpreted as an indicator of solid stress: the larger the opening, the greater the stress. Contrary to expectations based on clinical and pathological characteristics, this method indicated that human pancreatic neuroendocrine tumors and liposarcomas have the highest solid stress, whereas spheroids from human PDA cell lines had among the lowest (more precise estimates of solid stress could not be made because the bulk and shear moduli were unknown).<sup>21</sup> Taken at face value, neither the low estimated solid stress nor the low free IFP measured with the WN in pancreas cancer models<sup>11,41</sup> can explain the vascular collapse observed in autochthonous PDAs.

## Fluids, Solids, and Force Transmission

Force is transmitted differently through solids and fluids (Supplementary Figure 2). Force transmission through solids occurs only at the point of contact and parallel to the direction of the applied force (ie, vectorially). In fluids, force is transmitted uniformly in all directions (ie, hydraulically), a principle that underlies the widespread utility of hydraulics. Based on the classic methods and measurements described in the preceding text, a framework was put forth to describe the total tissue pressure as the sum of specific components of fluid pressures and solid pressures (Figure 4A). In this model, the gel-like fluid pressure was combined with the solid pressures that derive from insoluble fibers and cells. The free-fluid pressure arises from the kinetic energy of fluid molecules moving through the interstitial space. Solid stress is attributed to collagen fibers, elastin, the elastic gel, and other ECM components. However, solid tissue pressures are never distributed evenly because they are only exerted at sites of direct contact. A problem therefore arises in attempting to combine a force transmitted vectorially with one transmitted hydraulically, because not all structures and surfaces would be exposed to both pressures.<sup>32</sup> For these reasons, we propose a re-envisioning of the classic model in which the sources of pressure in the interstitium are based on the way they transmit force, rather than their ability to be measured by fluid equilibration techniques (Figure 4B). This concept also has the advantage of obviating any confusion over the precise physicochemical properties of a given component of the interstitium (ie, solid, fluid, or viscoelastic) while focusing on the most relevant parameter affecting vascular collapse in PDA.

## A Pressure by Any Other Name

What then is meant by a fluid pressure, and what do the WN and PC actually measure? We have previously referred to the pressures associated with fluid bound to interstitial HA (ie, the immobile or gel-fluid phase) as a fluid pressure.<sup>10</sup> Perhaps surprisingly, however, what precisely constitutes a solid and a fluid in tissues has been a matter of contention for decades (Figure 5). If we consider the interstitium to be a 2-phase system, then at steady state the sum of the hydrostatic and osmotic pressures in the free fluid will equal the sum of the hydrostatic and osmotic pressures in the gel-fluid phase (leaving aside concerns about the phenomenological constants for the moment) (Figure 6).<sup>32</sup> The PC measures the hydrostatic pressure in the gel phase, which includes multiple components, one of which is a relatively minor free-fluid portion that should be in equilibrium with the interstitial free-fluid pressure

that is captured by the WN and other fluid equilibration techniques. However, “(b) because collagen prevents the gel from swelling further, the fluid pressure in the gel always will be greater than the fluid pressure in any free-fluid in contact with the gel under equilibrium conditions.”<sup>13</sup>

In the end, attempts to define the precise mechanisms by which HA contributes to increased interstitial pressures may identify a problem in terminology and boil any debate down to semantics.<sup>13</sup> As Brace eloquently stated:

*Consider that the interstitial fluid is a heterogeneous mixture of gel and free fluid and is most frequently considered to be in two phases: a free fluid phase of relatively small volume and a gel fluid phase containing the major part of the tissue fluid. Does “interstitial fluid pressure” refer to the hydrostatic pressure in the free fluid or in the gel fluid? It has been used in reference to either the free fluid or the gel fluid phase or even to both without adequate distinction, despite the fact that theoretically the hydrostatic pressures in these two fluid phases are never equal.*<sup>13</sup>

If we restrict IFP to refer only to the pressure derived from free-flowing fluid, then the HA-bound fluid must be called something else. Labeling it a solid (Figure 5C) seems remiss, however, because this would overlook the essential and fluid-like manner in which it transmits pressure. Therefore, we propose that a solid tumor such as PDA is best described as a biphasic material composed of a freefluid phase and a viscoelastic, gel-fluid phase that has the force transmission properties of a fluid and the elastic properties of a solid (Figure 5B). The gel-fluid phase bridges the physiochemical gap between free fluid and true solids in the tissue interstitium. Together, these properties provide the only plausible mechanism for the widespread vascular collapse that occurs in PDA.

## Clinical Implications

Hyaluronidase, a naturally occurring enzyme that degrades HA, was originally identified as the spreading factor in bovine testes and later found to represent a glycoprophosphatidylinositol-linked enzyme on the acrosomal membrane of sperm that aided in fertilization.<sup>75</sup> The purified extract promoted fluid and solute resorption and increased diffusion in a number of experimental contexts.<sup>92–94</sup> Bovine testes hyaluronidase significantly increased the hydraulic conductivity of the pericardial stroma,<sup>95</sup> and direct intratumoral injection of bovine testes hyaluronidase decreased IFP measured by the WN and PC.<sup>10,73,96,97</sup> Early clinical trials involving subcutaneous injection of bovine testes hyaluronidase to enhance drug delivery had some success but were limited by cross-species immune reactions to the enzyme.<sup>94,98–102</sup> A recombinant form of the enzyme (rHuPH20) could efficiently remove HA in vitro, but its short half-life (<3 minutes) in vivo precluded its systemic use. Chemical conjugation of rHuPH20 with polyethylene glycol (PEG) created a product (PEGPH20) with greatly increased circulatory half-life (10.3 hours) and preserved enzymatic activity, making systemic delivery clinically tenable.<sup>10,12,73</sup> In *KPC* mice, the long half-life, coupled with at least a minority of accessible vasculature, led to significant catalytic degradation of intratumoral HA. HA depletion, in turn, resulted in a sharp decrease in IFP, expansion of the vasculature, and increased permeability to chemotherapeutics.<sup>10</sup>

PEGPH20 significantly increased the objective response rate and overall survival otherwise achievable in *KPC* mice with the deoxycytosine analogue gemcitabine alone.<sup>10,12</sup>

In a phase 1b trial of patients with metastatic PDA, PEGPH20 in combination with gemcitabine was well tolerated.<sup>103</sup> Although efficacy is not the primary objective in phase 1 studies, the investigators observed trends toward increased response rates and survival, particularly in patients with high intratumoral HA content in biopsy specimens collected before treatment. Moreover, infusional PEGPH20 increased perfusion ( $K_{trans}$ ), as measured by dynamic contrast-enhanced magnetic resonance imaging, and successfully ablated the target as assessed in posttreatment biopsy specimens.<sup>103</sup>

This basic strategy has now advanced to national, randomized trials involving the current standard of care regimens *nab*-paclitaxel + gemcitabine (NCT01839487) and FOLFIRINOX (NCT01959139). In an interim analysis of the trial of *nab*-paclitaxel + gemcitabine, with or without PEGPH20, patients with high intratumoral levels of HA had an objective response rate of 52% and progression-free survival of 9.2 months, compared with 23% and 4.3 months, respectively, in the chemotherapy alone group.<sup>104</sup> In patients with low intratumoral levels of HA, PEGPH20 did not improve the efficacy of chemotherapy, supporting its target-specific effects.

Despite the likely depletion of the low levels of HA in most organs, including heart, liver, lungs, and intestine, PEGPH20 appears to be generally well tolerated. The most common adverse effects are myalgias and arthralgias, which can be ameliorated with corticosteroids and tend to subside with time. An increase in thromboembolic events observed in the early phase of the trial has since been addressed and overcome with prophylactic low-molecular-weight heparin therapy.<sup>105</sup> A global randomized phase 3 trial of this strategy is now enrolling patients (NCT02715804).

Collectively, preclinical and clinical studies indicate that the notorious treatment resistance of PDA is due at least in part to the overproduction of HA, which creates excessive interstitial gel fluid pressures that can compress tumor vessels and block drug perfusion. Targeting the gel-fluid phase may similarly increase the efficacy of other agents previously considered ineffective against PDA and perhaps in other solid tumors as well.

## Conclusions

Most interstitial fluid in normal tissues is immobilized in complex with water-avid GAGs such as HA. The extremely high concentrations of HA secreted into the interstitium in PDA generate a large gel-fluid phase that profoundly alters the architecture, signaling, and fluid mechanics in the tumor. This gel-like fluid phase has a complex viscoelastic behavior and can generate multiple types of pressures. However, its ability to transmit applied pressures like a fluid (ie, hydraulically, or uniformly in all directions) is paramount to the widespread vascular collapse seen in PDA. The gel-fluid phase and associated swelling pressure of water bound to interstitial HA is the major determinant of vascular collapse and hypoperfusion in PDA; this pressure is counterpoised and augmented by a tethered collagen microfibrillary network.

These gel-fluid pressures were not fully appreciated until recently because of a lack of appropriate instruments and experimental platforms. There has also been an almost singular focus on the free-fluid pressures that exist in appreciable amounts only in certain physiological conditions, such as edema, and artificial model systems, such as transplantable tumor spheroids. Free-fluid pressures do not appear to contribute appreciably to the baseline biophysics and fluid mechanics in pancreas cancers and are therefore not the principal barrier to drug delivery. Targeted depletion of the principal driving force of increased fluid pressure, HA, reduces swelling pressure by mobilizing the bound fluid and alleviating vascular collapse. The resultant increase in perfusion and intratumoral drug delivery occurs despite not decreasing—and sometimes even increasing—the free-fluid pressures. This understanding reveals a primary mechanism of drug resistance in PDA, giving rise to a new strategy for approaching this intransigent disease and also inviting the intriguing prospect of rescuing agents previously believed to be ineffective. Turning attention to the role of the gel-fluid phase in other solid tumors may also be warranted.

## Supplementary Material

Refer to Web version on PubMed Central for supplementary material.

## Acknowledgments

The authors thank Martin Whittle and Shelley Thorsen for comments on the manuscript and Markus Carlson for assistance with figures.

### Funding

Supported by National Institutes of Health National Cancer Institute grant CA161112, the Lustgarten Foundation, the Giles W. and Elise G. Mead Foundation, and gifts from Maryanne Tagney and David Jones. The content is solely the responsibility of the authors and does not necessarily represent the official views of the National Institutes of Health.

## Abbreviations used in this paper

<b>ECM</b>	extracellular matrix
<b>GAG</b>	glycosaminoglycan
<b>HA</b>	hyaluronic acid
<b>IFP</b>	interstitial fluid pressure
<b>PC</b>	pressure catheter
<b>PDA</b>	pancreatic ductal adenocarcinoma
<b>PEG</b>	polyethylene glycol
<b>WN</b>	wick-in-needle

## References

1. Cancer facts & figures 2015. Atlanta, GA: American Cancer Society: American Cancer Society; 2015.



2. Hanahan D, Weinberg RA. Hallmarks of cancer: the next generation. *Cell*. 2011; 144:646–674. [PubMed: 21376230]
3. Hidalgo M. Pancreatic cancer. *N Engl J Med*. 2010; 362:1605–1617. [PubMed: 20427809]
4. Shields MA, Dangi-Garimella S, Redig AJ, et al. Biochemical role of the collagen-rich tumour microenvironment in pancreatic cancer progression. *Biochem J*. 2012; 441:541–552. [PubMed: 22187935]
5. Pandol S, Edderkaoui M, Gukovsky I, et al. Desmoplasia of pancreatic ductal adenocarcinoma. *Clin Gastroenterol Hepatol*. 2009; 7:S44–S47. [PubMed: 19896098]
6. Liotta LA, Kohn EC. The microenvironment of the tumour-host interface. *Nature*. 2001; 411:375–379. [PubMed: 11357145]
7. Bhowmick NA, Neilson EG, Moses HL. Stromal fibroblasts in cancer initiation and progression. *Nature*. 2004; 432:332–337. [PubMed: 15549095]
8. Tlsty TD, Coussens LM. Tumor stroma and regulation of cancer development. *Annu Rev Pathol*. 2006; 1:119–150. [PubMed: 18039110]
9. Olive KP, Jacobetz MA, Davidson CJ, et al. Inhibition of hedgehog signaling enhances delivery of chemotherapy in a mouse model of pancreatic cancer. *Science*. 2009; 324:1457–1461. [PubMed: 19460966]
10. Provenzano PP, Cuevas C, Chang AE, et al. Enzymatic targeting of the stroma ablates physical barriers to treatment of pancreatic ductal adenocarcinoma. *Cancer Cell*. 2012; 21:418–429. [PubMed: 22439937]
11. DelGiorno KE, Carlson MA, Osgood R, et al. Interstitial pressure and vascular collapse in pancreas cancer-fluids and solids, measurement and meaning. *Cancer Cell*. 2014; 26:16–17. [PubMed: 25026210]
12. Jacobetz MA, Chan DS, Nesses A, et al. Hyaluronan impairs vascular function and drug delivery in a mouse model of pancreatic cancer. *Gut*. 2013; 62:112–120. [PubMed: 22466618]
13. Brace RA. Progress toward resolving the controversy of positive vs. negative interstitial fluid pressure. *Circ Res*. 1981; 49:281–297. [PubMed: 7018732]
14. Michel, CC. Fluid movements through capillary walls. In: Renkin, EM.; Michel, CC., editors. *Handbook of physiology*. Vol. IV. Washington, DC: American Physiological Society; 1984. p. 375-409.
15. Ogston AG, Michel CC. General descriptions of passive transport of neutral solute and solvent through membranes. *Prog Biophys Mol Biol*. 1978; 34:197–217. [PubMed: 375302]
16. Jain RK. Transport of molecules across tumor vasculature. *Cancer Metastasis Rev*. 1987; 6:559–593. [PubMed: 3327633]
17. Staverman AJ. Non-equilibrium thermodynamics of membrane processes. *Trans Faraday Soc*. 1952; 48:176–185.
18. Kedem O, Katchalsky A. Thermodynamic analysis of the permeability of biological membranes to non-electrolytes. *Biochim Biophys Acta*. 1958; 27:229–246. [PubMed: 13522722]
19. Kedem O, Katchalsky A. A physical interpretation of the phenomenological coefficients of membrane permeability. *J Gen Physiol*. 1961; 45:143–179. [PubMed: 13752127]
20. Helmlinger G, Netti PA, Lichtenbeld HC, et al. Solid stress inhibits the growth of multicellular tumor spheroids. *Nat Biotechnol*. 1997; 15:778–783. [PubMed: 9255794]
21. Stylianopoulos T, Martin JD, Chauhan VP, et al. Causes, consequences, and remedies for growth-induced solid stress in murine and human tumors. *Proc Natl Acad Sci U S A*. 2012; 109:15101–15108. [PubMed: 22932871]
22. Sarntinoranont M, Rooney F, Ferrari M. Interstitial stress and fluid pressure within a growing tumor. *Ann Biomed Eng*. 2003; 31:327–335. [PubMed: 12680730]
23. Michel CC. Starling: the formulation of his hypothesis of microvascular fluid exchange and its significance after 100 years. *Exp Physiol*. 1997; 82:1–30. [PubMed: 9023503]
24. Starling EH. On the absorption of fluids from the connective tissue spaces. *J Physiol*. 1896; 19:312–326.
25. Starling EH. The arris and gale lectures on the physiological factors involved in the causation of dropsy. Lecture i. The production of lymph. *Lancet*. 1896; 1:1267–1270.

26. Starling EH. The arris and gale lectures on the physiological factors involved in the causation of dropsy. Lecture ii. The absorption of fluids from the connective tissue spaces. *Lancet*. 1896; 1:1331–1334.
27. Guyton AC, Granger HJ, Taylor AE. Interstitial fluid pressure. *Physiol Rev*. 1971; 51:527–563. [PubMed: 4950077]
28. Guyton AC. A concept of negative interstitial pressure based on pressures in implanted perforated capsules. *Circ Res*. 1963; 12:399–414. [PubMed: 13951514]
29. Scholander PF, Hargens AR, Miller SL. Negative pressure in the interstitial fluid of animals. Fluid tensions are spectacular in plants; in animals they are elusively small, but just as vital. *Science*. 1968; 161:321–328. [PubMed: 5661289]
30. Fadnes HO, Reed RK, Aukland K. Interstitial fluid pressure in rats measured with a modified wick technique. *Microvasc Res*. 1977; 14:27–36. [PubMed: 895543]
31. McMaster PD. The pressure and interstitial resistance prevailing in the normal and edematous skin of animals and man. *J Exp Med*. 1946; 84:473–494. [PubMed: 19871582]
32. Aukland K, Reed RK. Interstitial-lymphatic mechanisms in the control of extracellular fluid volume. *Physiol Rev*. 1993; 73:1–78. [PubMed: 8419962]
33. Guyton AC, Scheel K, Murphree D. Interstitial fluid pressure. 3. Its effect on resistance to tissue fluid mobility. *Circ Res*. 1966; 19:412–419. [PubMed: 5914853]
34. Young JS, Lumsden CE, Stalker AL. The significance of the tissue pressure of normal testicular and of neoplastic (brown-pearce carcinoma) tissue in the rabbit. *J Pathol Bacteriol*. 1950; 62:313–333. [PubMed: 14784896]
35. Brown WH, Pearce L. Neoplasia in experimental syphilis. *Exp Biol Med*. 1921; 18:201–202.
36. Jain RK. Transport of molecules in the tumor interstitium—a review. *Cancer Res*. 1987; 47:3039–3051. [PubMed: 3555767]
37. Provenzano PP, Hingorani SR. Hyaluronan, fluid pressure, and stromal resistance in pancreas cancer. *Br J Cancer*. 2013; 108:1–8. [PubMed: 23299539]
38. Roberts WG, Palade GE. Increased microvascular permeability and endothelial fenestration induced by vascular endothelial growth-factor. *J Cell Sci*. 1995; 108:2369–2379. [PubMed: 7673356]
39. Heldin CH, Rubin K, Pietras K, et al. High interstitial fluid pressure—an obstacle in cancer therapy. *Nat Rev Cancer*. 2004; 4:806–813. [PubMed: 15510161]
40. Hashizume H, Baluk P, Morikawa S, et al. Openings between defective endothelial cells explain tumor vessel leakiness. *Am J Pathol*. 2000; 156:1363–1380. [PubMed: 10751361]
41. Chauhan VP, Boucher Y, Ferrone CR, et al. Compression of pancreatic tumor blood vessels by hyaluronan is caused by solid stress and not interstitial fluid pressure. *Cancer Cell*. 2014; 26:14–15. [PubMed: 25026209]
42. Netti PA, Hamberg LM, Babich JW, et al. Enhancement of fluid filtration across tumor vessels: Implication for delivery of macromolecules. *Proc Natl Acad Sci U S A*. 1999; 96:3137–3142. [PubMed: 10077650]
43. Boucher Y, Baxter LT, Jain RK. Interstitial pressure-gradients in tissue-isolated and subcutaneous tumors—implications for therapy. *Cancer Res*. 1990; 50:4478–4484. [PubMed: 2369726]
44. Combest AJ, Roberts PJ, Dillon PM, et al. Genetically engineered cancer models, but not xenografts, faithfully predict anticancer drug exposure in melanoma tumors. *Oncologist*. 2012; 17:1303–1316. [PubMed: 22993143]
45. Nagy JA, Dvorak HF. Heterogeneity of the tumor vasculature: the need for new tumor blood vessel type-specific targets. *Clin Exp Metastasis*. 2012; 29:657–662. [PubMed: 22692562]
46. Ruzinova MB, Schoer RA, Gerald W, et al. Effect of angiogenesis inhibition by id1 loss and the contribution of bone-marrow-derived endothelial cells in spontaneous murine tumors. *Cancer Cell*. 2003; 4:277–289. [PubMed: 14585355]
47. Sikder H, Huso DL, Zhang H, et al. Disruption of id1 reveals major differences in angiogenesis between transplanted and autochthonous tumors. *Cancer Cell*. 2003; 4:291–299. [PubMed: 14585356]

48. Richmond A, Su Y. Mouse xenograft models vs GEM models for human cancer therapeutics. *Dis Model Mech.* 2008; 1:78–82. [PubMed: 19048064]
49. Becher OJ, Holland EC. Genetically engineered models have advantages over xenografts for preclinical studies. *Cancer Res.* 2006; 66:3355–3358. [PubMed: 16585152]
50. Sharpless NE, DePinho RA. Model organisms—the mighty mouse: genetically engineered mouse models in cancer drug development. *Nat Rev Drug Discov.* 2006; 5:741–754. [PubMed: 16915232]
51. Singh M, Ferrara N. Modeling and predicting clinical efficacy for drugs targeting the tumor milieu. *Nat Biotechnol.* 2012; 30:648–657. [PubMed: 22781694]
52. Hingorani SR, Petricoin EF, Maitra A, et al. Preinvasive and invasive ductal pancreatic cancer and its early detection in the mouse. *Cancer Cell.* 2003; 4:437–450. [PubMed: 14706336]
53. Hingorani SR, Wang LF, Multani AS, et al. Trp53(r172h) and kras(g12d) cooperate to promote chromosomal instability and widely metastatic pancreatic ductal adenocarcinoma in mice. *Cancer Cell.* 2005; 7:469–483. [PubMed: 15894267]
54. Aguirre AJ, Bardeesy N, Sinha M, et al. Activated kras and ink4a/arf deficiency cooperate to produce metastatic pancreatic ductal adenocarcinoma. *Genes Dev.* 2003; 17:3112–3126. [PubMed: 14681207]
55. Guerra C, Barbacid M. Genetically engineered mouse models of pancreatic adenocarcinoma. *Mol Oncol.* 2013; 7:232–247. [PubMed: 23506980]
56. Stromnes IM, DelGiorno KE, Greenberg PD, et al. Stromal reengineering to treat pancreas cancer. *Carcinogenesis.* 2014; 35:1451–1460. [PubMed: 24908682]
57. Guyton AC. Interstitial fluid pressure. II. Pressure-volume curves of interstitial space. *Circ Res.* 1965; 16:452–460. [PubMed: 14289154]
58. Laurent TC, Fraser JRE. Hyaluronan. *FASEB J.* 1992; 6:2397–2404. [PubMed: 1563592]
59. Toole BP. Hyaluronan: from extracellular glue to pericellular cue. *Nat Rev Cancer.* 2004; 4:528–539. [PubMed: 15229478]
60. Fessler JH. A structural function of mucopolysaccharide in connective tissue. *Biochem J.* 1960; 76:124–132. [PubMed: 13822561]
61. Hunger J, Bernecker A, Bakker HJ, et al. Hydration dynamics of hyaluronan and dextran. *Biophys J.* 2012; 103:L10–L12. [PubMed: 22828349]
62. Prusova A, Vergeldt FJ, Kucerik J. Influence of water content and drying on the physical structure of native hyaluronan. *Carbohydr Polym.* 2013; 95:515–521. [PubMed: 23618302]
63. Meyer, F. Distribution and transport of fluid as related to tissue structure. In: Hargens, A., editor. *Tissue nutrition and viability.* New York, NY: Springer-Verlag; 1986. p. 25-46.
64. Preston BN, Davies M, Ogston AG. The composition and physicochemical properties of hyaluronic acids prepared from ox synovial fluid and from a case of mesothelioma. *Biochem J.* 1965; 96:449–474. [PubMed: 5837786]
65. Katchalsky A. Polyelectrolyte gels. *Progr Biophys.* 1954; 4:1–59.
66. Katchalsky A. Polyelectrolytes and their biological interactions. *Biophys J.* 1964; 4(suppl):9–41. [PubMed: 14104085]
67. Ogston AG. On water binding. *Fed Proc.* 1966; 25:986–989. [PubMed: 5941026]
68. Tanford, C. *Physical chemistry of macromolecules.* New York: Wiley; 1961.
69. Krause WE, Bellomo EG, Colby RH. Rheology of sodium hyaluronate under physiological conditions. *Biomacromolecules.* 2001; 2:65–69. [PubMed: 11749156]
70. Zimmer HG, Millar HD. Technology and application of ultraminiature catheter pressure transducers. *Can J Cardiol.* 1998; 14:1259–1266. [PubMed: 9852939]
71. Ozerdem U, Hargens AR. A simple method for measuring interstitial fluid pressure in cancer tissues. *Microvasc Res.* 2005; 70:116–120. [PubMed: 16137719]
72. Simonsen TG, Gaustad J-V, Leinaas MN, et al. High interstitial fluid pressure is associated with tumor-line specific vascular abnormalities in human melanoma xenografts. *PLoS One.* 2012; 7:e40006. [PubMed: 22768196]

73. Thompson CB, Shepard HM, O'Connor PM, et al. Enzymatic depletion of tumor hyaluronan induces antitumor responses in preclinical animal models. *Mol Cancer Ther.* 2010; 9:3052–3064. [PubMed: 20978165]
74. Ozerdem U. Measuring interstitial fluid pressure with fiberoptic pressure transducers. *Microvasc Res.* 2009; 77:226–229. [PubMed: 18809414]
75. Balazs EA, Denlinger JL. Clinical uses of hyaluronan. *Ciba Found Symp.* 1989; 143:265–275. discussion 275–280, 281–285. [PubMed: 2680347]
76. Knudson CB, Knudson W. Hyaluronan-binding proteins in development, tissue homeostasis, and disease. *FASEB J.* 1993; 7:1233–1241. [PubMed: 7691670]
77. Turley EA, Noble PW, Bourguignon LYW. Signaling properties of hyaluronan receptors. *J Biol Chem.* 2002; 277:4589–4592. [PubMed: 11717317]
78. Toole BP. Hyaluronan-cd44 interactions in cancer: paradoxes and possibilities. *Clin Cancer Res.* 2009; 15:7462–7468. [PubMed: 20008845]
79. Bard, J. Developmental and cell biology series 23. Morphogenesis the cellular and molecular processes of developmental anatomy. Cambridge, England: Cambridge University Press; 1990.
80. Brinkley LL, Morris-Wiman J. Effects of chlorcyclizine-induced glycosaminoglycan alterations on patterns of hyaluronate distribution during morphogenesis of the mouse secondary palate. *Development.* 1987; 100:637–640. [PubMed: 2894970]
81. Bard JBL, Ross ASA. The morphogenesis of the ciliary body of the avian eye. 1. Lateral cell detachment facilitates epithelial folding. *Dev Biol.* 1982; 92:73–86. [PubMed: 7106389]
82. Bard JBL, Ross ASA. The morphogenesis of the ciliary body of the avian eye. 2. Differential enlargement causes an epithelium to form radial folds. *Dev Biol.* 1982; 92:87–96. [PubMed: 7106390]
83. Toole BP, Trelstad RL. Hyaluronate production and removal during corneal development in chick. *Dev Biol.* 1971; 26:28–35. [PubMed: 5111769]
84. Dvorak HF. Tumors: wounds that do not heal. Similarities between tumor stroma generation and wound healing. *N Engl J Med.* 1986; 315:1650–1659. [PubMed: 3537791]
85. DuFort CC, Paszek MJ, Weaver VM. Balancing forces: architectural control of mechanotransduction. *Nat Rev Mol Cell Biol.* 2011; 12:308–319. [PubMed: 21508987]
86. Frantz C, Stewart KM, Weaver VM. The extracellular matrix at a glance. *J Cell Sci.* 2010; 123:4195–4200. [PubMed: 21123617]
87. Oezdemir BC, Pentcheva-Hoang T, Carstens JL, et al. Depletion of carcinoma-associated fibroblasts and fibrosis induces immunosuppression and accelerates pancreas cancer with reduced survival. *Cancer Cell.* 2014; 25:719–734. [PubMed: 24856586]
88. Rhim AD, Oberstein PE, Thomas DH, et al. Stromal elements act to restrain, rather than support, pancreatic ductal adenocarcinoma. *Cancer Cell.* 2014; 25:735–747. [PubMed: 24856585]
89. Sherman MH, Yu RT, Engle DD, et al. Vitamin D receptor-mediated stromal reprogramming suppresses pancreatitis and enhances pancreatic cancer therapy. *Cell.* 2014; 159:80–93. [PubMed: 25259922]
90. Infinity Pharmaceuticals. Infinity reports update from phase 2 study of saridegib plus gemcitabine in patients with metastatic pancreatic cancer. 2012 <http://phx.corporate-ir.net/phoenix.zhtml?c=121941&p=irol-newsArticle&ID=1653550>.
91. Padera TP, Stoll BR, Tooredman JB, et al. Cancer cells compress intratumour vessels. *Nature.* 2004; 427:695–695. [PubMed: 14973470]
92. Beckenlehner K, Bannke S, Spruss T, et al. Hyaluronidase enhances the activity of adriamycin in breast-cancer models invitro and invivo. *J Cancer Res Clin Oncol.* 1992; 118:591–596. [PubMed: 1517281]
93. Kohno N, Ohnuma T, Truog P. Effects of hyaluronidase on doxorubicin penetration into squamous carcinoma multicellular tumor spheroids and its cell lethality. *J Cancer Res Clin Oncol.* 1994; 120:293–297. [PubMed: 8126058]
94. Smith KJ, Skelton HG, Turiansky G, et al. Hyaluronidase enhances the therapeutic effect of vinblastine in intralesional treatment of kaposi's sarcoma. *J Am Acad Dermatol.* 1997; 36:239–242. [PubMed: 9039176]

95. Sunnergren KP, Rovetto MJ. The effects of hyaluronidase on interstitial hydration, plasma protein exclusion, and microvascular permeability in the isolated perfused rat heart. *Microvasc Res.* 1985; 30:286–297. [PubMed: 3911032]
96. Zawieja DC, Garcia C, Granger HJ. Oxygen radicals, enzymes, and fluid transport through pericardial interstitium. *Am J Physiol.* 1992; 262:H136–H143. [PubMed: 1310233]
97. Brekken C, Davies CD. Hyaluronidase reduces the interstitial fluid pressure in solid tumours in a non-linear concentration-dependent manner. *Cancer Lett.* 1998; 131:65–70. [PubMed: 9839621]
98. Baumgartner G, Gomar-Hoss C, Sakr L, et al. The impact of extracellular matrix on the chemoresistance of solid tumors—experimental and clinical results of hyaluronidase as additive to cytostatic chemotherapy. *Cancer Lett.* 1998; 131:85–99. [PubMed: 9839623]
99. Pillwein K, Fuiko R, Slavic I, et al. Hyaluronidase additional to standard chemotherapy improves outcome for children with malignant brain tumors. *Cancer Lett.* 1998; 131:101–108. [PubMed: 9839624]
100. Maier U, Baumgartner G. Metaphylactic effect of mitomycin-c with and without hyaluronidase after transurethral resection of bladder-cancer—randomized trial. *J Urol.* 1989; 141:529–530. [PubMed: 2493098]
101. Klocker J, Sabitzer H, Raunik W, et al. Hyaluronidase as additive to induction chemotherapy in advanced squamous cell carcinoma of the head and neck. *Cancer Lett.* 1998; 131:113–115. [PubMed: 9839626]
102. Whatcott CJ, Han H, Posner RG, et al. Targeting the tumor microenvironment in cancer: why hyaluronidase deserves a second look. *Cancer Discov.* 2011; 1:291–296. [PubMed: 22053288]
103. Hingorani SR, Harris WP, Beck JT, et al. Phase Ib study of pegylated recombinant human hyaluronidase and gemcitabine in patients with advanced pancreatic cancer. *Clin Cancer Res.* 2016 Jan 26. [Epub ahead of print].
104. Hingorani SR, Harris WP, Hendifar AE, et al. High response rate and PFS with PEGPH20 added to nabpaclitaxel/gemcitabine in stage IV previously untreated pancreatic cancer patients with high-HA tumors: interim results of a randomized phase II study. *J Clin Oncol.* 2015; 33(suppl) abstr 4006.
105. Hingorani SR, Harris WP, Seery TE, et al. Interim results of a randomized phase II study of PEGPH20 added to nab-paclitaxel/gemcitabine in patients with stage IV previously untreated pancreatic cancer. *J Clin Oncol.* 2016; 34 abstr 439.

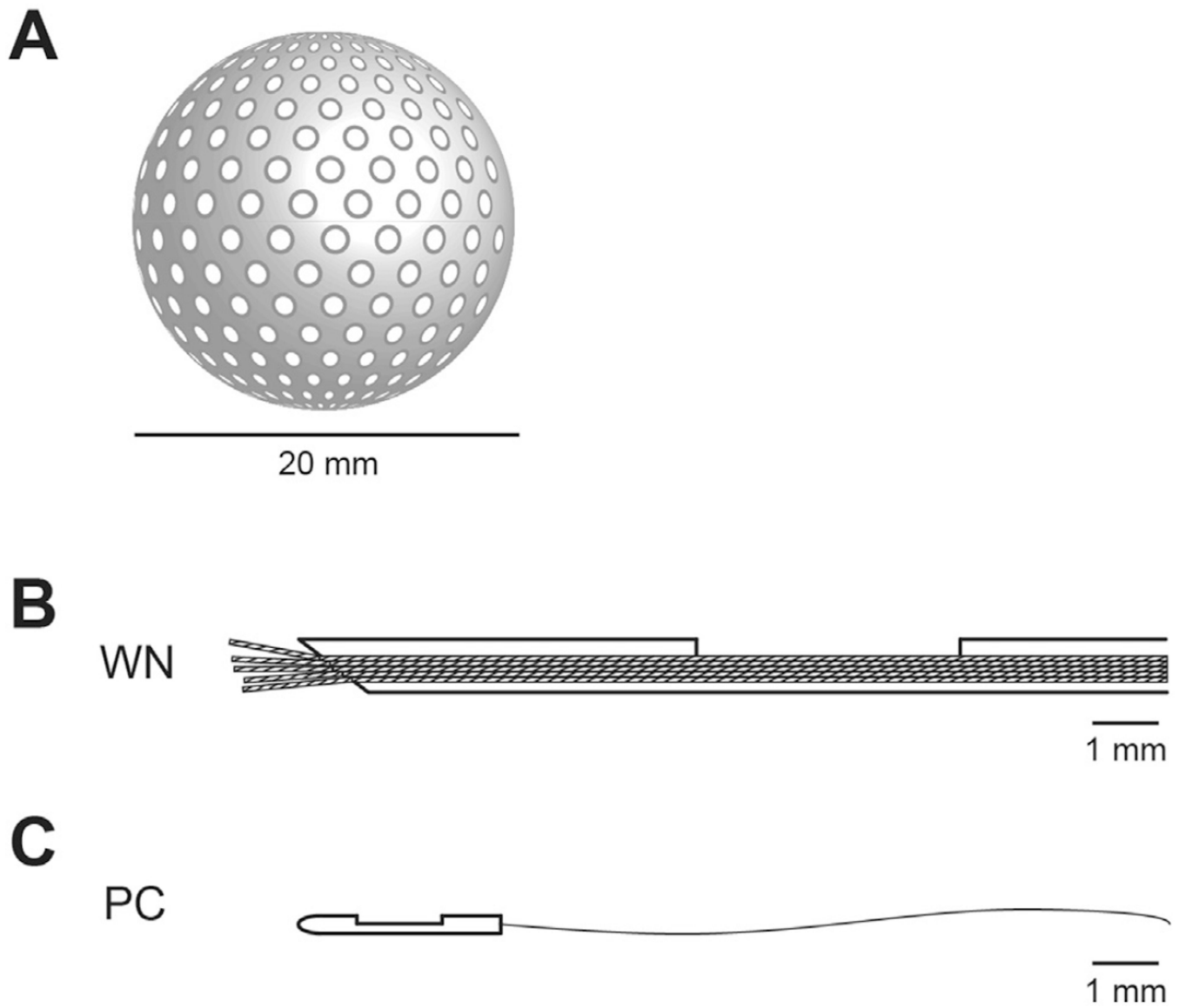


**Figure 1.**

IFP can be measured by a number of techniques. (A) Perforated capsules of 20 to 30 mm in diameter and varying shapes can be implanted into tissues and allowed to equilibrate over 2 to 3 weeks. The capsules fill with interstitial fluid and proteins, and the pressure can be measured by inserting a needle into the inner cavity. (B) The WN technique consists of a hypodermic needle (0.6 mm, outer diameter) with a ~3-mm-long side hole situated about 5 mm from the needle tip. Nylon fibers are pulled through the needle and connected through fluid-filled tubing to a pressure transducer. (C) The PC is the smallest probe, with a 0.33-mm outer diameter. It is optimized for measurements in the pressure range from  $-50$  the device is to  $+300$  mm Hg and is the only device capable of measuring pressures associated with the immobile (gel) fluid phase.



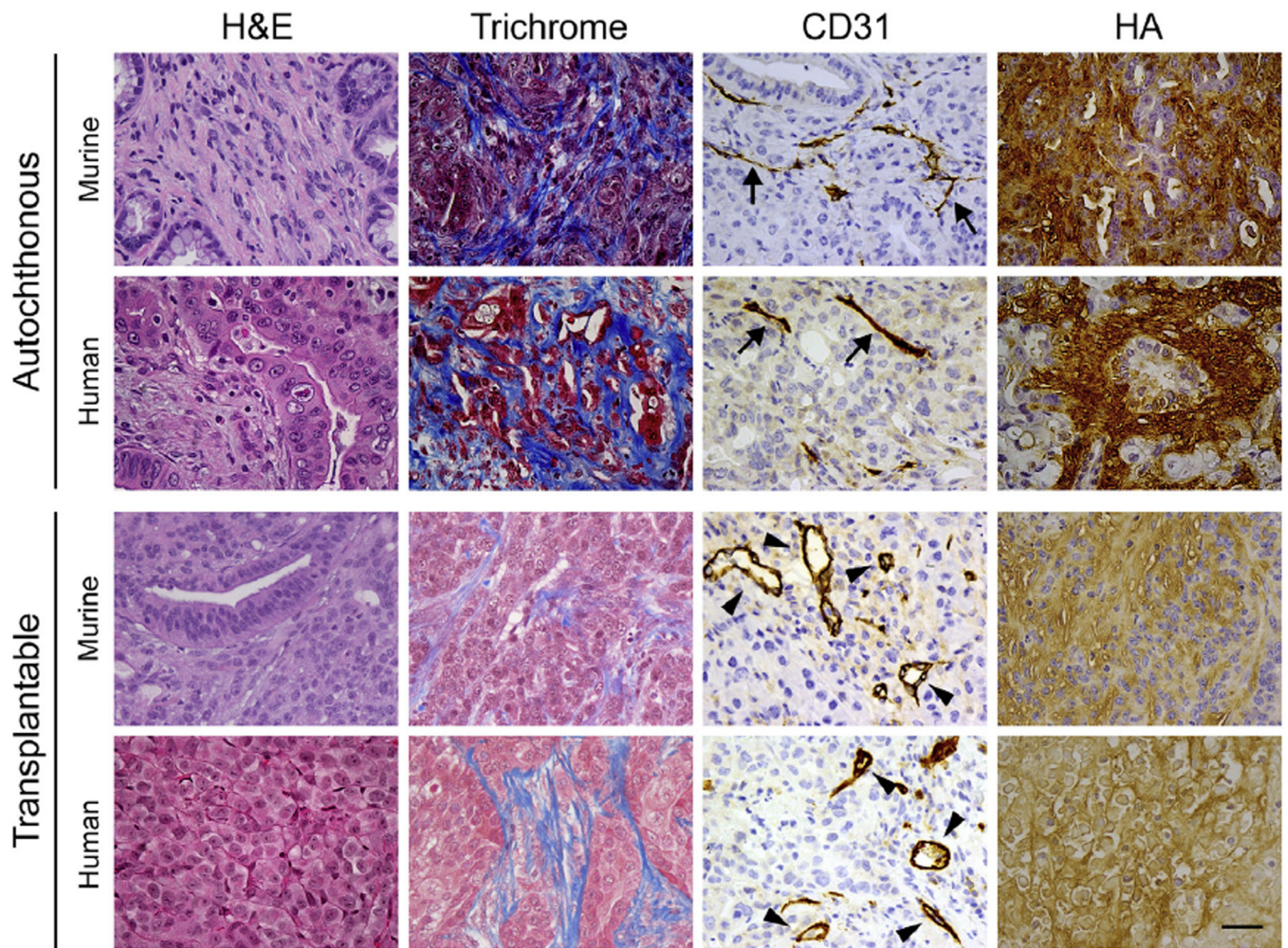


**Figure 2.**

Xenograft and allograft models do not faithfully recapitulate the epithelial or stromal properties of autochthonous tumors. Histologic and histochemical analyses of tumors from *KPC* mice and human PDA (autochthonous) compared with allograft and xenograft tumors from mice and human PDA cell lines, respectively (transplantable). Important differences can be seen in basic histological features (by H&E stain), total collagen content (trichrome), HA content, and vascular patency (CD31) showing collapsed vessels characteristic of autochthonous PDA (*arrows*) and patent vessels found in transplantable tumors (*arrowheads*). *Scale bar* = 25  $\mu$ m.

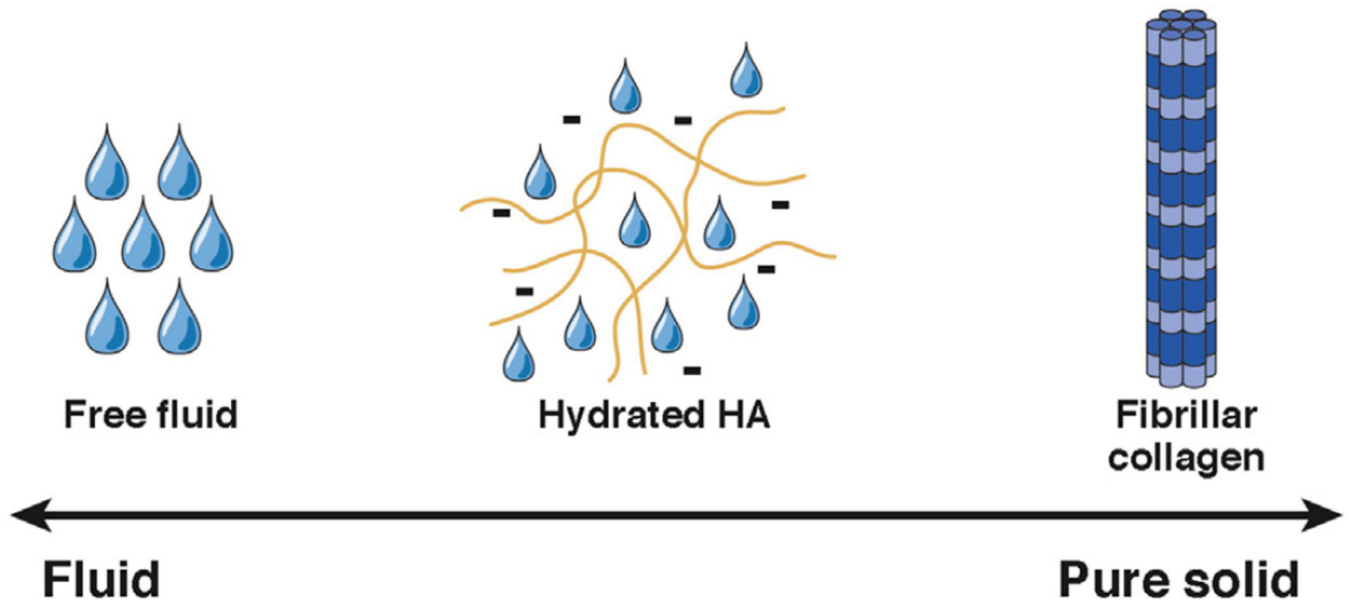


**Figure 3.** Determinants of interstitial pressure in pancreas cancer. Factors that contribute to interstitial pressure in PDA range from pure fluid to pure solid. Most pressure derives from a viscoelastic, HA-dominated, immobile gel-fluid phase that cannot be measured with conventional devices for measuring fluid pressure.

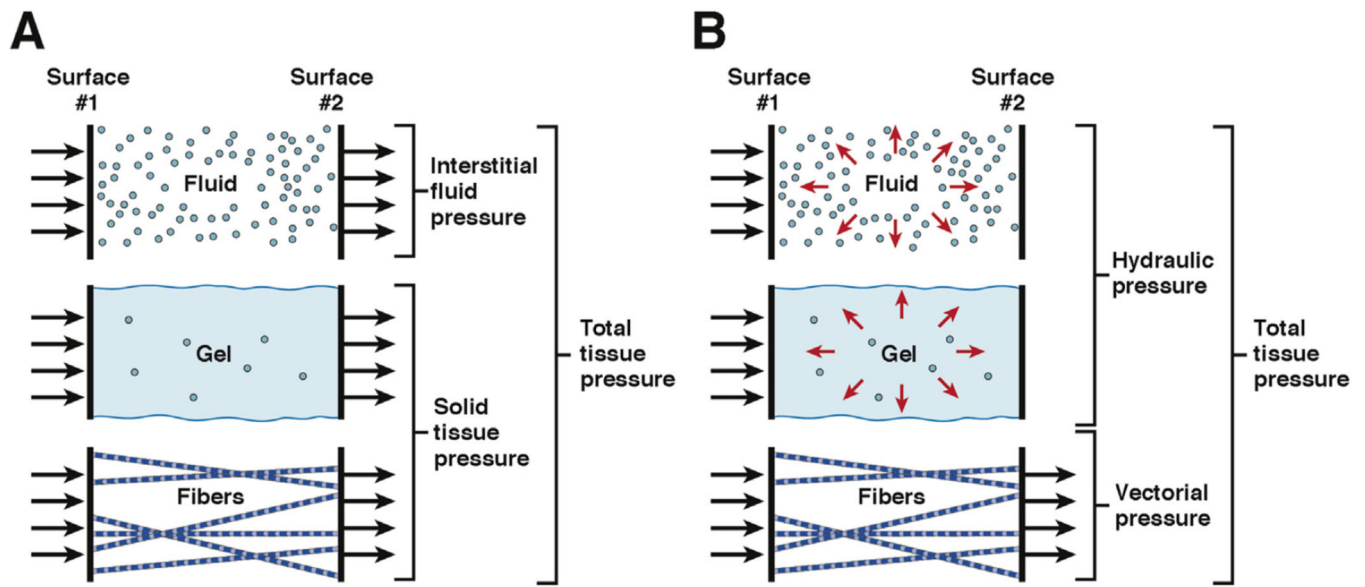


**Figure 4.**

Transmission of fluid, solid, and gel fluid pressures in tissues. (A) The classic depiction of tissue pressures (adapted from Guyton et al<sup>27</sup> with permission) considers 2 broad categories: fluid and solid. Gel fluid is categorized as a solid. (B) In an alternative model proposed here, pressure sources are instead described according to the manner in which they transmit force (ie, vectorially or hydraulically).



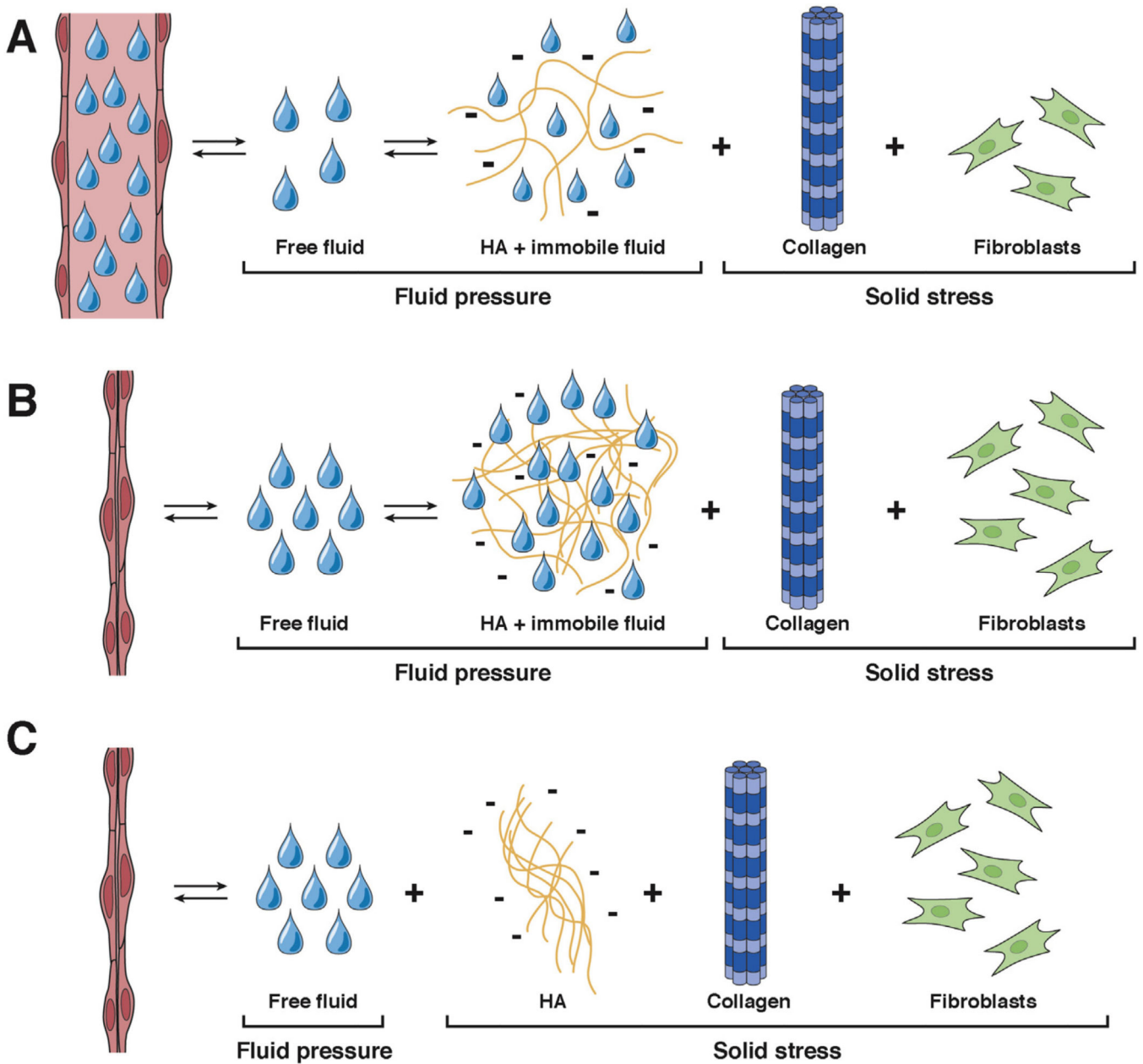


**Figure 5.**

Contributions of fluid and solid stress in normal tissue and PDA. (A) In normal tissues, pressures exerted on blood vessels are generated from the combination of IFP and solid stress from the ECM. Fluid pressures from free fluid and the HA-bound, gel-fluid phase are distinct from the pressures generated by solid elements such as collagen and fibroblasts in the stroma. Most interstitial fluid found in normal tissues is bound to HA and other GAGs. (B) The interstitial phase is greatly expanded in the transition from normal epithelium to preinvasive and invasive PDA. This transition is characterized by increased deposition of HA and other ECM components, culminating in an invasive disease with extremely high IFP and significant areas of vascular collapse. (C) A competing framework instead models HA as a solid element with IFP being generated solely by free fluid.

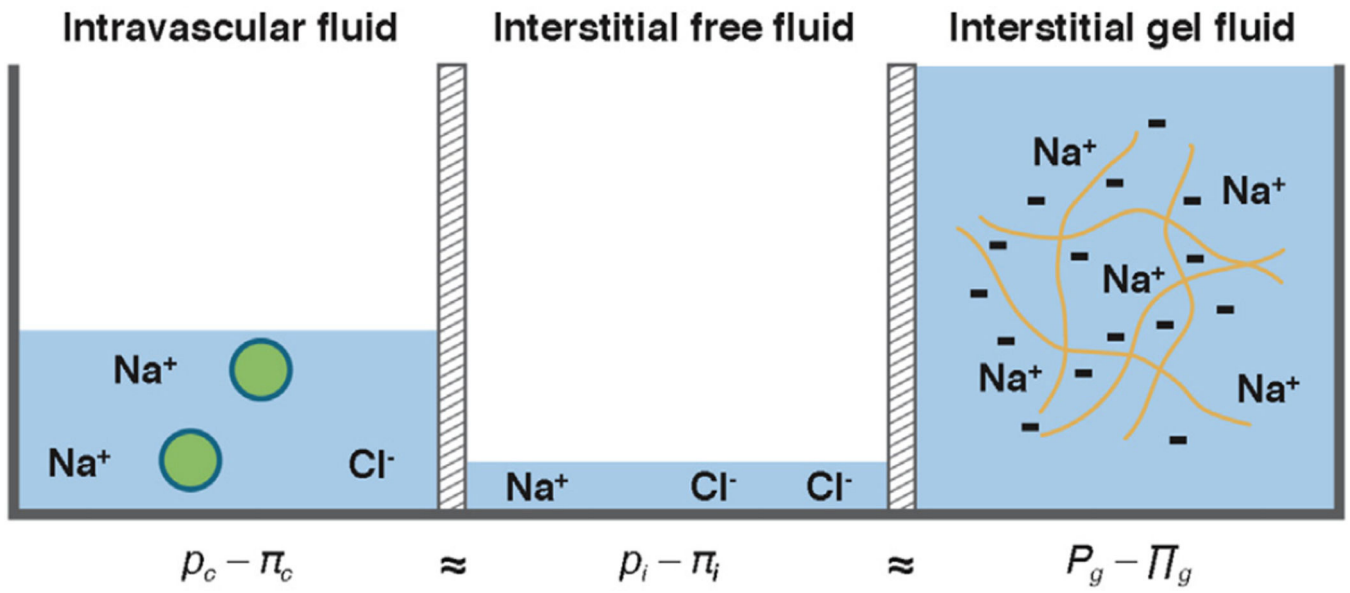


**Figure 6.**

Fluid pressures in the 2-phase model of the tissue interstitium. At steady state, the sum of the hydrostatic and osmotic fluid pressures in the intravascular (c), interstitial free fluid (i), and interstitial gel fluid (g) compartments are in equilibrium.